Active Galactic Nuclei Feedback and the Origin and Fate of the Hot Gas in Early-type Galaxies

Silvia Pellegrini[1] , Luca Ciotti[1] , Andrea Negri[2], and Jeremiah P. Ostriker[3]
[1] Department of Physics and Astronomy, University of Bologna, via Gobetti 93/2, I-40129 Bologna, Italy
[2] Instituto de Astrofísica de Canarias, calle Vía Láctea, E-38205 La Laguna, Tenerife, Spain
[3] Department of Astronomy, Columbia University, 550 West 120th Street, New York, NY 10027, USA
Received 2017 September 4; revised 2018 January 30; accepted 2018 February 6; published 2018 March 29

Abstract

A recent determination of the relationships between the X-ray luminosity of the ISM (L_X) and the stellar and total mass for a sample of nearby early-type galaxies (ETGs) is used to investigate the origin of the hot gas, via a comparison with the results of hydrodynamical simulations of the ISM evolution for a large set of isolated ETGs. After the epoch of major galaxy formation (after $z \simeq 2$), the ISM is replenished by stellar mass losses and SN ejecta, at the rate predicted by stellar evolution, and is depleted by star formation; it is heated by the thermalization of stellar motions, SNe explosions, and the mechanical (from winds) and radiative AGN feedback. The models agree well with the observed relations, even for the largely different L_X values at the same mass, thanks to the sensitivity of the gas flow to many galaxy properties; this holds for models including AGN feedback, and those without. Therefore, the mass input from the stellar population is able to account for a major part of the observed L_X; and AGN feedback, while very important to maintain massive ETGs in a time-averaged quasi-steady state, keeping low star formation and the black hole mass, does not dramatically alter the gas content originating in stellar recycled material. These conclusions are based on theoretical predictions for the stellar population contributions in mass and energy, and on a self-consistent modeling of AGN feedback.

Key words: galaxies: elliptical and lenticular, cD – galaxies: evolution – galaxies: kinematics and dynamics – quasars: supermassive black holes – X-rays: galaxies – X-rays: ISM

1. Introduction

In recent years our knowledge of the dynamical structure of early-type galaxies (hereafter ETGs), and of the properties of their hot interstellar medium, has improved considerably. On the one hand, estimates of the luminous and dark mass distributions have become possible out to large radii thanks to integral field spectroscopy and the use of mass tracers extending to many effective radii, such as globular clusters and planetary nebulae (e.g., Deason et al. 2012; Norris et al. 2012; Morganti et al. 2013; Napolitano et al. 2014; Cappellari et al. 2015; Alabi et al. 2016, 2017; Foster et al. 2016; Poci et al. 2017; see also Cappellari 2016). On the other hand, a large number of ETGs have had a significant exposure with the X-ray satellite *Chandra*, and the resulting data have been analyzed with uniform procedures by various groups, obtaining properties for the hot gas more accurately than ever; in particular, for the first time, the contribution of stellar sources to the total X-ray emission could be efficiently removed (e.g., Boroson et al. 2011; Kim & Fabbiano 2013, hereafter KF13, 2015; Su et al. 2015; Goulding et al. 2016).

The improved knowledge of the dynamical structure of ETGs and of their hot gas properties has been used to investigate the link between the total mass (stars+dark matter, M_t) and the hot gas luminosity (L_X) and temperature. In fact, it is expected that the gas content and temperature depend primarily on M_t being related, respectively, to the gas binding energy and virial temperature (e.g., Ciotti et al. 1991; David et al. 1991; Pellegrini 2011; Posacki et al. 2013; KF13). It was thus shown that indeed the total mass is the primary factor in retaining the hot gas. For a sample of 14 ETGs, the relation between L_X and the total mass within $5R_e$ (hereafter $M_{t,5R_e}$), where R_e is the optical effective radius, turned out to be tighter than that between L_X and the total

optical luminosity, especially for gas rich ETGs (KF13). For ETGs with $L_X <$ few $\times 10^{40}$ erg s^{-1}, the scatter in the relation suggests the importance of secondary factors, such as galaxy rotation, galaxy shape, star formation history, environment, AGN feedback. Forbes et al. (2017, hereafter F17) recently revisited the correlation between L_X of ETGs and various masses: the galaxy stellar mass ($M_\star$), $M_{t,5R_e}$, and M_t. They used homogeneous mass measurements for 29 galaxies from the SLUGGS survey, which provides kinematic information for stars (to a few R_e) and globular clusters (out to $\simeq 10R_e$) in two dimensions (Alabi et al. 2017). Consistently with the earlier results of KF13, they found a strong linear relationship between L_X and $M_{t,5R_e}$, confirming that the total mass is the primary factor in driving the hot gas content. F17 also compared their relationships to the predictions of SPH simulations of galaxy formation and subsequent evolution within the ΛCDM paradigm, where a major source for the ISM is provided by infall within dark matter halos of pristine gas, that is shock-heated to X-ray emitting temperatures. In particular, they found agreement with the results of Choi et al. (2015), for the set of simulations that include mechanical and radiation heating from AGN (while models without feedback, or with thermal feedback, show systematically higher X-ray luminosity than that observed, as already noted by Choi et al. 2015).

In another approach that makes use of hydrodynamical simulations, but of the "grid" type, the hot gas evolution is followed after the epoch of galaxy formation (Ciotti et al. 1991, 2017, hereafter C17; Negri et al. 2014, hereafter N14), starting with galaxies almost empty of ISM, due to the combined effects of the SNe explosions and of the AGNs that are believed to clear the galaxies from the residual ISM, and "quench" star formation (e.g., Silk & Rees 1998; Di Matteo et al. 2005, 2012; Debuhr et al. 2012; Dubois et al. 2013;

Vogelsberger et al. 2013; Khandai et al. 2015; Schaye et al. 2015; Barai et al. 2018; Bieri et al. 2017; DeGraf et al. 2017). The ISM is then replenished by the collective input provided by the stellar population during its normal ageing, via stellar mass losses and supernovae ejecta. This source of mass for the ISM is accurately predicted by the stellar evolution theory, and it is not minor (of the order of $\approx 10\%$ of $M_\star$; e.g., C17). The resulting ISM evolution has been investigated for a large set of representative galaxy models, varying their M_t, shape, internal kinematics, the presence of AGN feedback, and star formation (N14; Negri et al. 2015, hereafter N15; C17). Here we show how this modeling, at the present epoch, can account well for the relations presented by F17, with implications for the origin of the hot gas observed today, and the effect of AGN feedback.

The paper is organized as follows: In Section 2, we briefly describe the numerical simulations (main code properties, model galaxies, mass and energy input from the stellar population and the AGN). In Section 3, we present the resulting relations between the hot gas properties and the mass of the models on various scales and compare them with those obtained by F17 for observed ETGs. In Section 4, we discuss the results and present the conclusions.

2. The Models: Dynamical Structure, Stellar Population Inputs, and AGN Feedback

We very briefly describe here the main features of the modeling and of the numerical implementation adopted to describe the evolution of the hot ISM in ETGs in our recent works (see N14, N15, C17 for more details on the specific simulations used here, and Ciotti & Ostriker 2012 for a detailed description of the realization of all input sources and of AGN feedback).

High-resolution 2D hydrodynamical simulations, performed with the ZEUS MP2 code, have been run for a large set of underlying axisymmetric two-component (star+dark matter) galaxy models, with a central massive black hole (MBH), of shapes ranging from E0 to E7. The Jeans equations provide the internal stellar kinematics, ranging from that of the isotropic rotator to the fully anisotropic case, on which the stellar kinematical heating is then based (N14). The stellar density profile follows a deprojected (ellipsoidal) Sérsic law, and the main observables (galaxy luminosity L, R_e, central stellar velocity dispersion) are related to lie on the main scaling laws. The spherical dark matter halo has a radial profile predicted by cosmological simulations (Navarro et al. 1997), and is normalized to account for a dark-to-stellar mass ratio of $M_h/M_\star \simeq 20$ (e.g., Behroozi et al. 2013), and for a dark mass within R_e lower than the stellar mass, as measured in the local universe (e.g., Cappellari et al. 2015). With respect to ETGs of the local universe, the galaxy models built in this way are the most realistic ones adopted so far in hydrodynamical simulations (Posacki et al. 2013; N14); they are kept fixed during the time span of the simulations. We do not account for the possibility of galaxy merging; this is a less severe approximation than it might seem, though, because the stellar dynamical time and the sound crossing time are comparable. Thus, the most conspicuous effects of the merging on the stellar structure and gas dynamics fade away within ≈ 1–2 Gyr, a fiducial virialization time.

The hot gas originates from stellar mass losses and SN ejecta, and evolves under the action of gravity, of cooling, and

of various energy sources: SNe explosions, thermalization of the random and ordered kinetic energy of stellar motions, and accretion onto the central MBHs, when present. The mass and energy input from the ageing stellar population are secularly declining, according to the prescriptions of stellar evolution theory for the "normal" stellar mass losses, and, for the SN Ia rate, to the predictions of progenitors evolution and to survey observations extending to medium redshift (e.g., Pellegrini 2012). Note that this modeling is still valid even in the presence of gas-poor merging, because the added galaxy will contribute with its own stellar population inputs. Star formation is also included, via a simple scheme based on physical arguments shown to reproduce the Kennicutt–Schmidt relation well (N15); cold gas is removed from the numerical grid due to star formation, and SNe II produced by the newly born stellar population are also considered as sources of mass and energy (see Ciotti & Ostriker 2012 for a thorough description of the mass and energy inputs from the old, secularly evolving stellar population and the newly born one, and of their realization in the code).

C17 followed the evolution of hot gas flows, including an accurate and physically self-consistent implementation of AGN feedback, both radiative and mechanical; the latter is due to AGN winds (as observed for BAL AGNs and high-redshift quasars, e.g., Tombesi 2016; Zakamska et al. 2016). The adopted grid modeling allows for a high resolution of the hydrodynamical fields over the whole extent of the galaxy; with a logarithmic grid spacing, the central resolution is 5 pc, which is inside the fiducial accretion radius (e.g., Pellegrini 2010; Ciotti & Pellegrini 2017), and the outermost radius is 250 kpc. Moreover, the heating of the ISM by AGN feedback results from the mass accretion rate on the MBH computed with a high central resolution, a self-consistent treatment of the mass, energy and momentum balance of the inflowing and outflowing material at the first radial gridpoint (Ostriker et al. 2010), and radiative and mechanical efficiencies, including their variation with the mass accretion rate, in agreement with current observational and theoretical findings. Sub-grid physics (i.e., accretion on a free-fall time) applies only to the innermost gridpoint, inside the accretion radius. In conclusion, we do not resort to assumptions to determine the mass accretion rate (as, e.g., a "boost factor"; Booth & Schaye 2009; Dubois et al. 2015), and we cannot adjust the "strength" of AGN feedback, since the heating of the ISM resulting from the accretion process is self-determined.

Each galaxy evolves in isolation, and at the beginning of the simulation is assumed to be $\simeq 2$ Gyr old, an age after which the prescriptions for the stellar population inputs are accurate and reliable (e.g., Pellegrini 2012); this epoch can be placed at around $z \simeq 2$, since the bulk of the stellar population of ETGs is old (e.g., Renzini 2006; Prichard et al. 2017). At the beginning, the galaxies are also assumed to be devoid of gas, as a result of outflows powered by SNe and/or quasars that ended the high star formation epoch (Section 1). The simulations follow the ISM evolution for the subsequent 11 Gyr, thus ending at a galaxy age of $\simeq 13$ Gyr.

For comparison with the X-ray observations and mass determinations in F17, we consider here two sets of models, of shapes ranging from E0 to E4 and E7: the first set includes models without AGN feedback (N14; N15; C17), and the internal kinematics for the E4 and E7 shapes may or may not include rotation; the second set contains models with
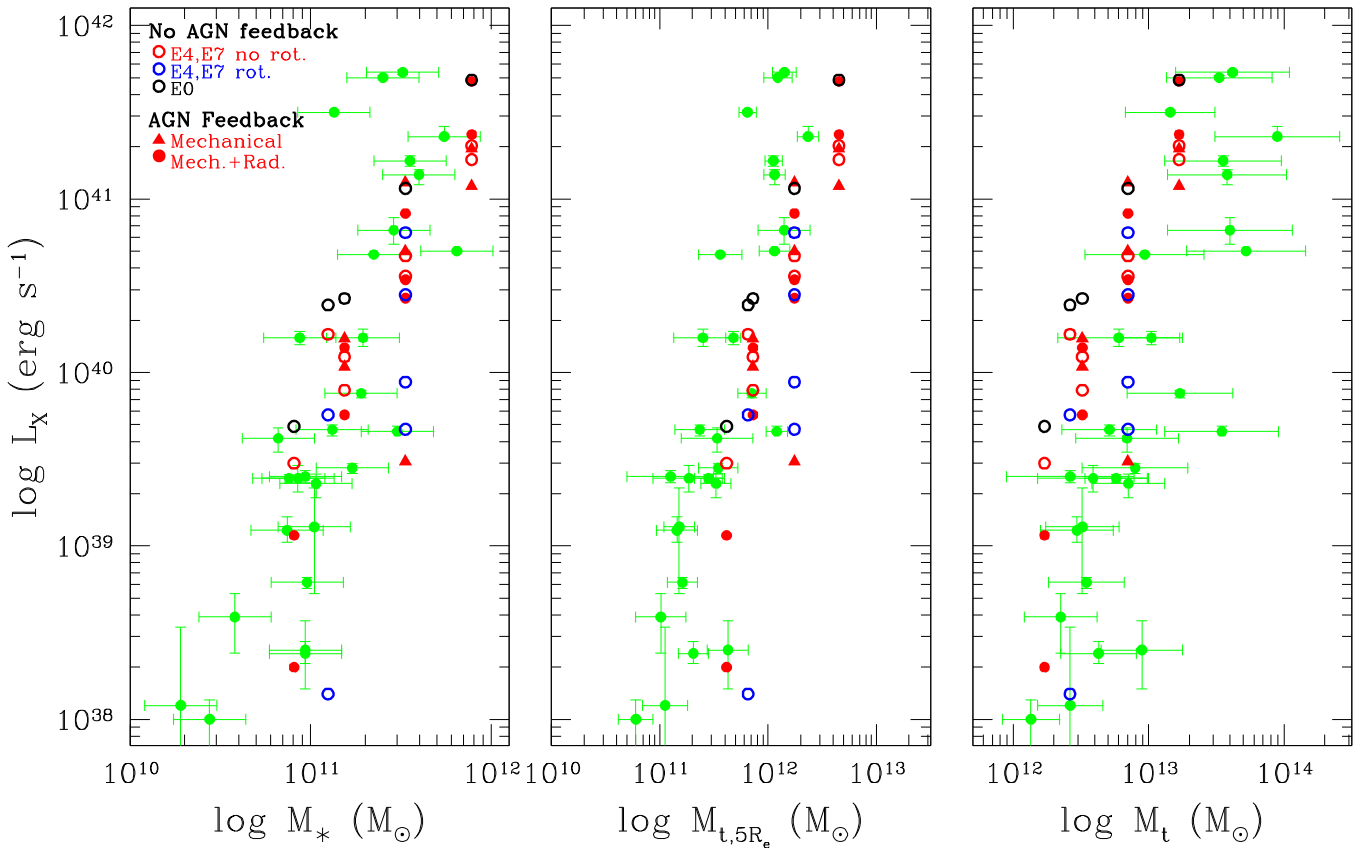
Figure 1. Observed (green) and model X-ray luminosities vs. the total stellar mass $M_\star$ (left), the total enclosed mass within $5R_e$ $M_{t,5R_e}$ (middle), and the total virial mass M_t (right). For observed ETGs, X-ray luminosities and masses are taken from F17, who derived stellar+dark masses from globular cluster kinematics (Section 3). The models have E0, E4, and E7 shapes; full symbols refer to nonrotating galaxies with AGN feedback (mechanical, or mechanical and radiative); open symbols refer to simulations without AGN feedback, and in this case the E4 and E7 galaxies can be rotating (blue open circles) or not (red open circles). The internal kinematics of rotating models is that of isotropic rotators; for $M_\star = 3.35 \times 10^{11} M_\odot$ also two cases with a lower rotational level are plotted (these have the largest L_X among rotating models at this $M_\star$; N15). See Section 2 for more details and references for the models.

AGN feedback (mechanical or radiative+mechanical), and the simulations have been performed for nonrotating galaxies (C17). The role of AGN feedback in rotating galaxies is under investigation. All details about the galaxy models and their X-ray properties are given in the references above.

3. The Models in the L_X–Mass Plots

Figure 1 shows the present-epoch values of L_X for the set of model galaxies described in Section 2, versus the various masses considered by F17: the total stellar mass $M_\star$, the total mass within $5R_e$ ($M_{t,5R_e}$), and the total galaxy mass M_t. The X-ray emission, in the energy band of 0.3–8 keV, comes from a sphere of $5R_e$ radius, an extraction region typically used in observational works; it includes almost all of L_X in models and observations.

Figure 1 has been built for a direct comparison of the models with the results of F17, thus it mimics exactly Figure 2 of F17. The green points with errorbars show the F17 sample of observed ETGs, all within a distance of 27 Mpc. For these ETGs, L_X over 0.3–8 keV comes mostly from the analysis of *Chandra* data conducted by KF13 and Kim & Fabbiano (2015), and has been extracted from galaxy radii that vary from 2 to 5 R_e. The dynamical masses within $5R_e$ derive from the Globular Clusters kinematics of the SLUGGS survey (Alabi et al. 2017); the total virial masses M_t are calculated by

extrapolating from $M_{t,5R_e}$, assuming an NFW-like dark matter halo. While definitely minor within R_e (Cappellari et al. 2015), the dark matter fraction within $5R_e$ shows a range of values (from ∼0.1 to 0.9), for $M_\star \gtrsim 10^{11} M_\odot$ (Alabi et al. 2017); between $5R_e$ and the virial radius there is practically only dark mass. Thus, the dark mass resides mostly outside the region where the bulk of the stellar recycled material is produced. Finally, the ETGs in the sample of F17 lie in a variety of environments, from the field to the group to the cluster. Only two of them are central dominant galaxies in clusters (M87, not shown in Figure 1 for its large L_X, and NGC 1399); other two are optically luminous ETGs at the center of their groups (NGC 5846 and NGC 1407).

3.1. General Comparison with Observations

The left panel shows that L_X of the models reproduces well the distribution of observed values, at all the $M_\star$ of the simulations ($M_\star = 0.81, 1.25, 1.54, 3.35, 7.80 \times 10^{11} M_\odot$). From the lowest to the largest $M_\star$, the following main features of the hot gas flow allow us to account for the observed L_X. Models of the lowest $M_\star$ ($M_\star \lesssim 1.2 \times 10^{11} M_\odot$) host a significant outflow/wind region, mostly SN-driven (as already established previously; e.g., Pellegrini & Ciotti 1998; David et al. 2006; Pellegrini et al. 2007) and then their L_X remains low; indeed, a few of the models at these lower $M_\star$ have

$L_X < 10^{38}$ erg s^{-1}, and then they do not appear in the plot. For $M_\star = 1.2 \times 10^{11} M_\odot$, only models without AGN feedback have been run, yet their L_X ranges from 1.4×10^{38} erg s^{-1} to 2.7×10^{40} erg s^{-1}, and is able to cover the large L_X interval observed at this $M_\star$. For $M_\star \geqslant 1.5 \times 10^{11} M_\odot$, all models have $L_X >$ a few $\times 10^{39}$ erg s^{-1}, due to the increasing binding energy of the gas with increasing galaxy mass (e.g., Pellegrini 2012; Posacki et al. 2013). The most systematically explored mass is $M_\star = 3.3 \times 10^{11} M_\odot$, where the models examine the effects of all the major galaxy properties (shapes from E0 to E7, with and without rotation); again, L_X spans from 3×10^{39} erg s^{-1} to 2×10^{41} erg s^{-1}, and covers most of the very large observed range. At fixed galaxy mass, L_X is lower for flatter morphologies, because the outflowing region is larger (N14); L_X is also lower in rotating ETGs, since rotation creates a cold disk and reduces L_X (N14, N15). The largest observed L_X values[4] of a few $\times 10^{41}$ erg s^{-1} are reproduced by the models with $M_\star = 7.4 \times 10^{11} M_\odot$. Note how the range of observed L_X tends to narrow at the largest $M_\star$, a property that is shown also by the models. In the models, this is explained in part by the exclusion of flat and rotating galaxies, because the most massive ETGs tend to be round and nonrotating; and in part by the progressive reduction of the size of an outflowing region as the galaxy mass increases. In summary, previous models available in the literature, not tailored specifically for comparison with the F17 results, appear to naturally account for the observed trend of L_X with $M_\star$ of F17. The large variation in L_X accomplished by the models at the same $M_\star$ lies in the sensitivity of the gas flow to many factors characterizing ETGs, as galaxy shape, presence of rotation, presence of star formation, and AGN feedback.

The agreement between the models and the results of F17 remains good also in the other two panels of Figure 1, where the x-axis includes the dark mass; the latter already provides a dominant contribution within $5R_e$ (middle panel). The models seem to have $M_{t,5R_e}$ slightly larger than derived for the sample of observed ETGs, for the same $M_\star$ (middle panel), while they tend to have M_t lower than evaluated from extrapolation of the inner mass profile by F17 (right panel). However, note that a mismatch of the size in Figure 1 between the amount and distribution of dark matter in the models and in the estimates of F17 is not expected to make L_X resulting from the simulations unreliable; in fact, the region important for determining L_X is the inner few R_e, where the stellar mass dominates and the models have been built with the correct fraction of dark matter (Section 2, N14). Moreover, the total mass estimates of F17 would imply that the gas should be slightly less bound than in the models, within $5R_e$, but more bound on the largest scale; thus, it is not straightforward to predict whether and in what sense L_X of the models would change, when inserting exactly the F17 estimates.

3.2. What is the Role of AGN Feedback?

Here we give a closer inspection of Figure 1 at the $M_\star$ values for which models with and without AGN feedback have been run (full and open symbols respectively), to understand whether there is a difference in their relative distribution. At the lowest $M_\star = 8.1 \times 10^{10} M_\odot$, the models in general host large outflowing regions, due to the SNe heating, even without AGN feedback; the effect of the latter is that of making the loss of gas easier, and then of a further decrease of L_X. For larger $M_\star \geqslant 1.5 \times 10^{11} M_\odot$, the range of L_X covered by the three types of models (no AGN feedback, mechanical feedback, and radiative+mechanical feedback) is similar, at each $M_\star$; there is no clear tendency of one type to occupy preferentially lower or larger L_X values. The only feature common at all $M_\star$ is that spherical models without AGN feedback are always found at the top of the distribution of L_X values.

The similarity of L_X shown by models with and without AGN feedback is the result of two important properties of the secular gas flow evolution. The first is that the outburst episodes triggered by accretion on the MBH are very brief: during the outbursts, L_X of the hot gas becomes very high, mostly due to a central bright and hot region, but, after a few $\times 10^7$ years, L_X quickly drops, and most of the time remains at normal, "quiescent" values (C17). For example, during the past 3–5 Gyr, the fraction of time spent above an L_X representative of a large gas emission observed for local ETGs ($L_X = 3 \times 10^{41}$ erg s^{-1}; Figure 1) is just $\approx 1\%$ (C17; Pellegrini et al. 2012). The second feature important to understand the similarity of L_X in models with and without AGN feedback is the actual effect of the latter on the gas flow on the galactic scale. After the first $\simeq 2$ Gyr of life of ETGs, during the epoch that is simulated, adding AGN feedback produces an increase in the ejected mass from the galaxy of the order of 20%–40%, going, respectively, from the largest to the smallest modeled ETGs; AGN feedback is not capable of producing a global major outflow by itself. Recurrent feedback helps to temporarily displace the gas from the center (out to a radius of $\lesssim 10$ kpc), thus temporarily reducing L_X even considerably, but it does not clear the whole galaxy from the gas. The net result is a comparable X-ray emission in present-day ETGs that have evolved with or without AGN feedback.

Even though it does not dramatically alter the overall hot gas content, AGN feedback produces a big difference in the amount of gas accreted to the center over the galaxies' lifetime, with important astrophysical consequences: during the galaxy evolution after $z \simeq 2$, it maintains ETGs in a time-averaged quasi-steady state, and keeps central star formation and the MBH mass low, by suppressing recurrent "cooling flows." For example, feedback is crucial to obtain final MBH masses close to the values observed (C17): in models without AGN feedback, the final MBH mass is far larger than that measured in the local universe (e.g., in the Magorrian et al. 1998 relation). In the feedback models, instead, after most of the MBH mass has grown by the end of the quasar epoch, as in the Soltan argument, just $\lesssim 3\%$ of the total injected mass from stars is accreted on the MBH, during the simulations, and the average increase in the MBH mass is just a factor of a few. In summary, in lower mass ETGs ($M_\star \lesssim 10^{11} M_\odot$), most of the injected stellar mass loss is expelled in an outflow, driven mainly by SNIa's explosions (as already known; e.g., Ciotti et al. 1991; Pellegrini & Ciotti 1998); in models of larger mass, roughly half of the total mass losses since an age of $\simeq 2$ Gyr ends recycled into new stars,[5] and the other half goes for a minor fraction into the MBH, and for a major fraction is ejected from the galaxy, due to SN heating and the further help of the AGN feedback action.

---

[4] The two largest observed L_X in Figure 1 belong to NGC 1399 and NGC 5846, two "central" ETGs (Section 3), while the models refer to isolated ETGs. For central galaxies, an intracluster/intragroup medium can produce a confinement effect that increases L_X.

[5] The AGN feedback has also a positive action for the formation of new stars, which is currently referred to as "positive feedback" (Ciotti & Ostriker 2007).

4. Discussion and Conclusions

We have compared a recent determination of the relations between the observed L_X and the stellar and total mass, for a sample of local ETGs (F17), with the L_X values at the present epoch of our hydrodynamical modeling of the hot gas evolution in ETGs. The model galaxies are isolated and devoid of ISM at the beginning, as expected after the "quenching" phase that ended the major star formation process. The ISM is then replenished in mass according to the prescriptions of the stellar evolution theory. With respect to previous numerical investigations of the fate of the recycled stellar material in ETGs, this work has two objectives: (1) to examine the possibility for the stellar input to account for a major part of the observed L_X, based on the comparison of the model results at the present epoch with the new, abovementioned relations; and (2) to clarify the possibility to use the present-day L_X as diagnostic of the impact of AGN activity, within a scenario where the hot gas mostly originates from the stellar population. To achieve these scopes, we considered a large set of galaxy models, built to have the present-day structural and kinematical properties observed for ETGs. We remark that the model predictions are based on high-resolution grid-type simulations, on a self-consistent computation of the mass accretion rate and of the heating of the gas due to AGN feedback, and on a contribution of stellar evolution reproducing the prescriptions of theory (see, e.g., the secular behavior of the mass losses from the ageing stellar population, and of the SNe Ia explosions; the inclusion of star formation from the cooling hot gas, with mass and energy return from the newly born stellar population, including SNe II).

We have found a good agreement between the L_X–$M_\star$ relation of the models and that of observed ETGs, over the whole $M_\star$ range. In particular, the largely different observed L_X values at the same $M_\star$ are reproduced by the sensitivity of the gas flow to many properties characterizing ETGs, as galaxy shape, presence of rotation, presence of star formation, and AGN feedback. The models also show an overall agreement with the observed L_X–$M_{t,5R_e}$ relation, though $M_{t,5R_e}$ of the models is slightly larger than that derived by F17, for ETGs of the same $M_\star$. The agreement between models and observations holds with and without radiative and mechanical (from AGN winds) AGN feedback. These results imply that the mass input from the stellar population is able to account for a large part of the observed L_X, and that—under the assumptions of this work—AGN feedback does not have a significant role in determining the present epoch L_X. This is an important conclusion about the fate of recycled stellar material in the presence of AGN feedback, since an outcome of the simulations could have been, for example, a major degassing of the galaxies. Such a different outcome would have implied the necessity to assume other sources of mass (as gas accretion from outside).

F17 noticed a good agreement between their results and the predictions of cosmological SPH simulations, where the hot gas mostly originates from a cosmological reservoir from which gas falls into the dark matter halos, is shock-heated, and is then further significantly heated by mechanical feedback due to AGN winds (Choi et al. 2015). If this mechanical feedback is not included, the simulations predict an L_X far larger than that observed; thus, it is concluded that the AGN plays an important role in determining L_X (in addition to M_t). This conclusion is not in contradiction with the results of the present work, which starts after $z \simeq 2$, and indicates that the AGN has not shaped dramatically the value of L_X observed today. In fact the cosmological simulations of Choi et al. (2015) as of many others (see, e.g., Section 1), start from the galaxy formation epoch, and obtain at early times AGN-driven powerful outflows that remove nearly all the gas, and stop star formation. In this sense, the role of the AGN is certainly very important. Our simulations (N14, N15, C17) start from these "initial conditions" created at the epoch of quenching, and find that at later epochs the energy injected by the AGN is not crucial in determining L_X of the recycled material (while fundamental to stop the recurrent cooling flow and keep the MBH mass low). The conclusions of the two approaches, one including and the other excluding the epoch of galaxy formation and the presence of cosmological gas, then agree, provided that AGN feedback in the first approach is stronger than that found here. In fact, if AGN-driven outflows are to clear the gas out of massive ETGs at early epochs and/or prevent a substantial cosmological accretion, this requires an efficiency of energy transfer from the AGN to the ISM much larger than that found by C17 at low redshift, when AGN feedback is not even able to clear the galaxies from the stellar mass losses. It could be that AGN feedback at the epoch of galaxy formation was stronger, perhaps due to a denser and more optically thick gas, and a shallower galactic potential well.

Finally, we discuss further the different origin of the hot gas, in the stellar population or in the cosmological infall. The input of mass considered in our simulation, from supernovae and stellar winds, including their secular trend, and both for the ageing and the newly born stars, is the minimum to be included for ETGs. The question then is how much infall can be accomodated at low redshift to still reproduce the observed L_X. If cosmological infall is very important, contributing to a mass within a few R_e much larger than that provided by stars, then the effects of AGN feedback should again be stronger than those found by C17, to obtain L_X of the values observed, MBH masses of the correct size, and limit star formation (see also Eisenreich et al. 2017). One possibility could be to include the additional effect of a jet, even though it is expected to represent the bulk of the energetic output when the Eddington-scaled mass accretion rate falls below a low threshold (of $\simeq 0.01$, Yuan & Narayan 2014). Indeed, this scaled rate seems to be low at the present epoch; for example, in the models of C17 it keeps below $\approx 10^{-3}$ for $\approx 75\%$ of the time after $z \simeq 2$, and it has been found similarly low in observational studies (Pellegrini 2005, 2010; Gallo et al. 2010). Jets are invoked to moderate the central cooling of the ISM, and of the intracluster medium (e.g., McNamara & Nulsen 2007; Heckman & Best 2014). How exactly the jet heating of the ISM works is still not very well understood; however, the present results suggest that, for isolated ETGs, radiative plus mechanical (from AGN winds) feedback already allows us to obtain L_X as observed, MBH masses on the Magorrian relation, and the correct low level of star formation (N15, C17). Further work, including the confining action exerted by an intragroup/intracluster medium, or cosmological infall, would be helpful to assess more thoroughly the origin of the hot gas and the role of AGN feedback in ETGs.

ORCID iDs

Silvia Pellegrini ⓘ https://orcid.org/0000-0002-8974-2996
Luca Ciotti ⓘ https://orcid.org/0000-0002-5708-5274
Jeremiah P. Ostriker ⓘ https://orcid.org/0000-0002-6405-9904

References

Alabi, A. B., Forbes, D. A., Romanowsky, A. J., et al. 2016, MNRAS, 460, 3838
Alabi, A. B., Forbes, D. A., Romanowsky, A. J., et al. 2017, MNRAS, 468, 3949
Barai, P., Gallerani, S., Pallottini, A., et al. 2018, MNRAS, 473, 4003
Behroozi, P. S., Wechsler, R. H., & Conroy, C. 2013, ApJ, 770, 57
Bieri, R., Dubois, Y., Rosdahl, J., et al. 2017, MNRAS, 464, 1854
Booth, C. M., & Schaye, J. 2009, MNRAS, 398, 53
Boroson, B., Kim, D. W., & Fabbiano, G. 2011, ApJ, 729, 12
Cappellari, M. 2016, ARA&A, 54, 597
Cappellari, M., Romanowsky, A. J., Brodie, J. P., et al. 2015, ApJL, 804, L21
Choi, E., Ostriker, J. P., Naab, T., Oser, L., & Moster, B. P. 2015, MNRAS, 449, 4105
Ciotti, L., D'Ercole, A., Pellegrini, S., & Renzini, A. 1991, ApJ, 376, 380
Ciotti, L., & Ostriker, J. P. 2007, ApJ, 665, 1038
Ciotti, L., & Ostriker, J. P. 2012, in Hot Interstellar Matter in Elliptical Galaxies, Astrophyics and Space Science Library, Vol. 378 ed. D.-W. Kim & S. Pellegrini (Berlin: Springer), 83
Ciotti, L., & Pellegrini, S. 2017, ApJ, 848, 29
Ciotti, L., Pellegrini, S., Negri, A., & Ostriker, J. P. 2017, ApJ, 835, 15 (C17)
David, L. P., Forman, W., & Jones, C. 1991, ApJ, 369, 121
David, L. P., Jones, C., Forman, W., Vargas, I. M., & Nulsen, P. 2006, ApJ, 653, 207
Deason, A. J., Belokurov, V., Evans, N. W., & McCarthy, I. G. 2012, ApJ, 748, 2
Debuhr, J., Quataert, E., & Ma, C.-P. 2012, MNRAS, 420, 2221
DeGraf, C., Dekel, A., Gabor, J., & Bournaud, F. 2017, MNRAS, 466, 1462
Di Matteo, T., Khandai, N., DeGraf, C., et al. 2012, ApJL, 745, L29
Di Matteo, T., Springel, V., & Hernquist, L. 2005, Natur, 433, 604
Dubois, Y., Gavazzi, R., Peirani, S., & Silk, J. 2013, MNRAS, 433, 3297
Dubois, Y., Volonteri, M., Silk, J., et al. 2015, MNRAS, 452, 1502
Eisenreich, M., Naab, T., Choi, E., Ostriker, J. P., & Emsellem, E. 2017, MNRAS, 468, 751
Forbes, D. A., Alabi, A., Romanowsky, A. J., et al. 2017, MNRAS, 464, L26 (F17)
Foster, C., Pastorello, N., Roediger, J., et al. 2016, MNRAS, 457, 147
Gallo, E., Treu, T., Marshall, P. J., et al. 2010, ApJ, 714, 25
Goulding, A. D., Greene, J. E., Ma, C.-P., et al. 2016, ApJ, 826, 167
Heckman, T. M., & Best, P. N. 2014, ARA&A, 52, 589
Khandai, N., Di Matteo, T., Croft, R., et al. 2015, MNRAS, 450, 1349
Kim, D.-W., & Fabbiano, G. 2013, ApJ, 776, 116 (KF13)
Kim, D.-W., & Fabbiano, G. 2015, ApJ, 812, 127
Magorrian, J., Tremaine, S., Richstone, D., et al. 1998, AJ , 115, 2285
McNamara, B. R., & Nulsen, P. E. J. 2007, ARA&A, 45, 117
Morganti, L., Gerhard, O., Coccato, L., et al. 2013, MNRAS, 431, 3570
Napolitano, N. R., Pota, V., Romanowsky, A. J., et al. 2014, MNRAS, 439, 659
Navarro, J. F., Frenk, C. S., & White, S. D. M. 1997, ApJ, 490, 493
Negri, A., Pellegrini, S., & Ciotti, L. 2015, MNRAS, 451, 1212 (N15)
Negri, A., Posacki, S., Pellegrini, S., & Ciotti, L. 2014, MNRAS, 445, 1351 (N14)
Norris, M. A., Gebhardt, K., Sharples, R. M., et al. 2012, MNRAS, 421, 1485
Ostriker, J. P., Choi, E., Ciotti, L., Novak, G., & Proga, D. 2010, ApJ, 722, 642
Pellegrini, S. 2005, ApJ, 624, 155
Pellegrini, S. 2010, ApJ, 717, 640
Pellegrini, S. 2011, ApJ, 738, 57
Pellegrini, S. 2012, in Hot Interstellar Matter in Elliptical Galaxies, Astrophysics and Space Science Library, Vol. 378 ed. D.-W. Kim & S. Pellegrini (Berlin: Springer), 21
Pellegrini, S., Baldi, A., Kim, D. W., Fabbiano, G., et al. 2007, ApJ, 667, 731
Pellegrini, S., & Ciotti, L. 1998, A&A, 333, 433
Pellegrini, S., Ciotti, L., & Ostriker, J. P. 2012, ApJ, 744, 21
Poci, A., Cappellari, M., & McDermid, R. M. 2017, MNRAS, 467, 1397
Posacki, S., Pellegrini, S., & Ciotti, L. 2013, MNRAS, 433, 2259
Prichard, L. J., Davies, R. L., Beifiori, A., et al. 2017, ApJ, 850, 203
Renzini, A. 2006, ARA&A, 44, 141
Schaye, J., Crain, R. A., Bower, R. G., et al. 2015, MNRAS, 446, 521
Silk, J., & Rees, M. J. 1998, A&A, 331, L1
Su, Y., Irwin, J. A., White, R. E., III, & Cooper, M. C. 2015, ApJ, 806, 156
Tombesi, F. 2016, AN, 337, 410
Vogelsberger, M., Genel, S., Sijacki, D., et al. 2013, MNRAS, 436, 3013
Yuan, F., & Narayan, R. 2014, ARA&A, 52, 529
Zakamska, N. L., Hamann, F., Pâris, I., et al. 2016, MNRAS, 459, 3144